

Direct Binding to Rsp5 Mediates Ubiquitin-independent Sorting of Sna3 via the Multivesicular Body Pathway^V

Matthew W. McNatt, Ian McKittrick, Matthew West, and Greg Odorizzi

Molecular, Cellular, and Developmental Biology, University of Colorado, Boulder, CO 80309-0347

Submitted August 1, 2006; Revised November 29, 2006; Accepted November 30, 2006

Monitoring Editor: Jean Gruenberg

The sorting of most integral membrane proteins into the luminal vesicles of multivesicular bodies (MVBs) is dependent on the attachment of ubiquitin (Ub) to their cytosolic domains. However, Ub is not required for sorting of Sna3, an MVB vesicle cargo protein in yeast. We show that Sna3 circumvents Ub-mediated recognition by interacting directly with Rsp5, an E3 Ub ligase that catalyzes monoubiquitination of MVB vesicle cargoes. The PPAY motif in the C-terminal cytosolic domain of Sna3 binds the WW domains in Rsp5, and Sna3 is polyubiquitinated as a consequence of this association. However, Ub does not appear to be required for transport of Sna3 via the MVB pathway because its sorting occurs under conditions in which its ubiquitination is impaired. Consistent with Ub-independent function of the MVB pathway, we show by electron microscopy that the formation of MVB vesicles does not require Rsp5 E3 ligase activity. However, cells expressing a catalytically disabled form of Rsp5 have a greater frequency of smaller MVB vesicles compared with the relatively broad distribution of vesicles seen in MVBs of wild-type cells, suggesting that the formation of MVB vesicles is influenced by Rsp5-mediated ubiquitination.

INTRODUCTION

Multivesicular bodies (MVBs) are late endosomes containing luminal vesicles that are formed by invagination of the endosomal membrane. The luminal MVB vesicles are delivered into the hydrolytic interior of the lysosome upon fusion of the limiting MVB membrane with the lysosomal membrane (van Deurs *et al.*, 1995; Futter *et al.*, 1996; Mullock *et al.*, 1998). Many cell-surface receptors that undergo down-regulation from the plasma membrane are sorted into MVB vesicles en route to being degraded in the lysosome, including members of the receptor tyrosine kinase family in metazoans and G protein-coupled receptors in the budding yeast *Saccharomyces cerevisiae*. In yeast, many biosynthetic proteins are also sorted into MVB vesicles during their transport from the Golgi to the vacuole, the functional equivalent of the lysosome (reviewed in Hicke and Dunn, 2003).

Most integral membrane proteins require the attachment of a single ubiquitin (Ub) to their cytosolic domains in order to be sorted into the MVB pathway (Katzmann *et al.*, 2001; Reggiori and Pelham, 2001; Urbanowski and Piper, 2001). Sorting of monoubiquitinated MVB cargoes is mediated by a highly conserved machinery comprised of class E Vps proteins, many of which assemble into distinct endosomal sorting complexes required for transport (ESCRTs) that contain Ub-binding domains (reviewed in Hurley and Emr, 2006). In addition to Ub-mediated cargo recognition, class E Vps pro-

teins are generally required for MVB vesicle budding because cells in which class E Vps proteins are disrupted contain malformed late endosomes that lack luminal vesicles (Rieder *et al.*, 1996; Odorizzi *et al.*, 1998; Doyotte *et al.*, 2005).

The class E Vps/ESCRT machinery is also required for the budding of many nonlytic enveloped viruses from infected host cells, which is topologically equivalent to the budding of MVB vesicles. Class E Vps proteins are recruited by virally encoded proteins that contain amino acid sequences known as “late domains” (reviewed in Morita and Sundquist, 2004). For example, the human immunodeficiency virus-1 Gag protein contains two late domains: the P(T/S)AP sequence, which binds the Tsg101 subunit of ESCRT-I, and the YP_x_nL sequence, which binds Alix. Rous sarcoma virus and many other viruses have the PPxY late domain, which is a consensus binding site for WW domains (Macias *et al.*, 2002). Viral PPxY late domains bind WW domains of the Nedd4 family of E3 Ub ligases, but the mechanistic role of Nedd4 proteins in viral budding is not clear (Morita and Sundquist, 2004).

Rsp5 is a Nedd4 homolog in yeast required for ubiquitination and sorting of most MVB cargo proteins (Blondel *et al.*, 2004; Dunn *et al.*, 2004; Hettema *et al.*, 2004; Katzmann *et al.*, 2004; Morvan *et al.*, 2004). Sna3, however, is a biosynthetic cargo that does not require Rsp5 activity in order to be sorted into MVB vesicles (Katzmann *et al.*, 2004), nor does it require Ub-binding functions of class E Vps proteins (Bilodeau *et al.*, 2002). Nevertheless, MVB sorting of Sna3 is dependent on general functions of the class E Vps machinery (Reggiori and Pelham, 2001; Yeo *et al.*, 2003; Katzmann *et al.*, 2004). In mammalian cells, Ub-independent MVB cargo sorting can occur in a manner that is either dependent on class E Vps proteins (Tanowitz and Von Zastrow, 2002; Hislop *et al.*, 2004) or independent of the class E Vps machinery (Theos *et al.*, 2006). Thus, multiple mechanisms sort cargo proteins via the MVB pathway. Here, we show that MVB sorting of Sna3 is mediated by a PPxY sequence in its

This article was published online ahead of print in *MBC in Press* (<http://www.molbiolcell.org/cgi/doi/10.1091/mbc.E06-08-0663>) on December 20, 2006.

^V The online version of this article contains supplemental material at *MBC Online* (<http://www.molbiolcell.org>).

Address correspondence to: Greg Odorizzi (odorizzi@colorado.edu).

Abbreviations used: ESCRT, endosomal sorting complex required for transport; MVB, multivesicular body; Ub, ubiquitin; Vps, vacuolar protein sorting.

Table 1. Yeast strains used in this study

Strain	Genotype	Reference
SEY6210	<i>MATα leu2-3,112 ura3-56 his3Δ200 trp1-Δ901 lys2-Δ801 suc2-Δ9</i>	Robinson <i>et al.</i> (1988)
TVY1	SEY6210; <i>pep4Δ::LEU2</i>	Wurmser and Emr (1998)
GOY100	SEY6210; <i>leu2-3,112::pBHY11 doa4^{C5715}</i>	This study
MWY6	GOY100; <i>pep4Δ::kanMX6</i>	This study
MMY161	TVY1; <i>SNA3-GFP::kanMX6</i>	This study
MMY64	MWY6; <i>SNA3-HA::HIS3</i>	This study
MMY153	MWY6; <i>sna3Δ::HIS3</i>	This study
<i>mob326</i>	<i>MATα leu2-3,112 ura3-56 his3Δ200 trp1Δ-901 ade2-Δ101 suc2-Δ9; <i>rsp5^{G555D}</i></i>	Katzmann <i>et al.</i> (2004)
MMY127	<i>MATα ade2-Δ101 SNA3-HA::HIS3 pep4Δ::kanMX6 doa4^{C5715} <i>rsp5^{G555D}</i></i>	This study
MMY157	MMY127; <i>tul1Δ::TRP1</i>	This study
GOY155	MWY6; <i>tul1Δ::HIS3</i>	This study
GOY157	MWY6; <i>bsd2Δ::HIS3</i>	This study
MMY56	SEY6210; <i>bsd2Δ::HIS3</i>	This study
MMY107	SEY6210; <i>sna3Δ::kanMX6</i>	This study
GW003	<i>MATα ade2-1 his3-11 ura3-1 trp1-1 can1-100 <i>rsp5Δ::LEU2</i></i>	Wang <i>et al.</i> (2001)

cytosolic domain that binds directly to the WW domains of Rsp5.

MATERIALS AND METHODS

Yeast Strains and Plasmid Constructions

Standard protocols were used for manipulations of *S. cerevisiae* (Guthrie and Fink, 2002) and for DNA manipulations using *Escherichia coli* (Sambrook and Russell, 2001). All plasmids constructions were confirmed by DNA sequence analysis. See Table 1 for the genotypes of yeast strains used in this study. Gene deletions and chromosomal integrations of epitope tags in yeast were constructed by homologous recombination of site-specific cassettes amplified by the PCR (Longtine *et al.*, 1998). The *doa4^{C5715}* allele from pGO309 (Luhtala and Odorizzi, 2004) was subcloned into pRS306 (Sikorski and Hieter, 1989), resulting in plasmid pGO311, and then integrated into the genome of BYH10 (Horadzovsky *et al.*, 1994) by homologous recombination (Guthrie and Fink, 2002) using pGO311 that had been linearized by restriction digestion, resulting in GOY100.

Site-directed mutagenesis of pSNA3-GFP (Katzmann *et al.*, 2004) resulting in codon substitutions in SNA3 yielded pMM158 (K₁₉R), pMM152 (K₁₂₅R), pMM159 (K₁₉R plus K₁₂₅R; referred to as K₀ in Figure 2A), pMM172 (P₁₀₆A), pMM99 (P₁₀₇L), and pMM171 (Y₁₀₉A). A PCR product corresponding to SNA3 codons 64-133 was subcloned into vector pET-His PL (Lykke-Andersen *et al.*, 2000) to yield pMM143 encoding His₆-Sna3^{CT} for expression in *E. coli*. Site-directed mutagenesis of pMM143 resulting in codon substitutions in SNA3 yielded pMM168 (P₁₀₆A), pMM154 (P₁₀₇L), pMM169 (Y₁₀₉A), pMM204 (A₁₀₈P), and pMM205 (A₁₀₈Q). PCR products corresponding to RSP5 codons 228-426 (WW123), codons 228-292 (WW1), codons 278-378 (WW2), or codons 377-426 (WW3) were subcloned into pGEX 4T1 (GE Healthcare, Waukesha, WI), resulting in pIM2, pIM6, pIM10, and pIM8, respectively. The WxxP motif in each WW domain was subsequently subjected to site-directed mutagenesis to replace the tryptophan with phenylalanine (W/F), resulting in pIM35 (in WW1), pIM36 (in WW2), and pIM37 (in WW3), or both the tryptophan with phenylalanine and the proline with alanine (W/F, P/A), resulting in pIM38 (in WW1), pIM39 (in WW2), and pIM40 (in WW3).

Preparation of Cell Extracts and Western Blotting

Yeast cell extracts were prepared from strains grown to OD₆₀₀ 0.5–0.8 and then harvested by centrifugation for 5 min at 500 × *g*, resuspended in 10 mM N-ethylmaleimide, and precipitated by the addition of 10% (vol/vol) trichloroacetic acid. After 10 min on ice, samples were isolated by centrifugation at 4°C for 10 min at 14,000 × *g* and then resuspended by sonication into ice-cold acetone. Samples were centrifuged and sonicated into ice-cold acetone again and centrifuged once more as described above, and then the pellets were dried by centrifugation under vacuum, resuspended by sonication into protein sample buffer (62.5 mM Tris-HCl, pH 6.8, 2% SDS, 5% 2-mercaptoethanol, 10% glycerol, 0.01% bromophenol blue), and 0.5 OD₆₀₀ units were resolved by SDS-PAGE.

For Western blotting, commercially available mouse monoclonal antibodies were used to detect the green fluorescence protein (GFP; Hoffman-La Roche, Nutley, NJ), the hemagglutinin epitope (HA; Zymed, South San Francisco, CA), and yeast 3-phosphoglycerate kinase (PGK; Invitrogen, Carlsbad, CA). Rabbit polyclonal antisera was used to detect yeast carboxypeptidase S (CPS; Cowles *et al.*, 1997), and yeast Doa4. The anti-Doa4 antiserum was commer-

cially prepared (Invitrogen) by coinjection of three peptide conjugates corresponding to amino acids 115-130, 620-635, and 894-909 of Doa4.

Fluorescence Microscopy

GFP, DsRed, and FM 4-64 fluorescence and differential interference contrast (DIC) microscopy was performed using a DMRXA microscope (Leica, Deerfield, IL) equipped with a Cooke Sensicam digital camera (Applied Scientific Instrumentation, Eugene, OR). Images were deconvolved using Slidebook 4.0 software (Intelligent Imaging Innovations, Denver, CO), and processed using Adobe Photoshop 7.0 software (Adobe Systems, San Jose, CA). Cells were stained with FM 4-64 (Invitrogen) using a pulse-chase procedure as described previously (Odorizzi *et al.*, 2003).

Electron Microscopy

Cells were grown to logarithmic phase, then high-pressure frozen, freeze-substituted with 0.1% uranyl acetate, 0.25% glutaraldehyde, anhydrous acetone at –90°C, and embedded in Lowicryl HM20 (Polysciences, Warrington, PA) and subsequently polymerized under UV at –50°C (Winey *et al.*, 1995). Thin sections (~70 nm) were prepared by microtomy and examined on a Phillips CM10 transmission electron microscope (TEM; Mahwah, NJ) at 80 kV. For electron tomography, 200-nm semithick sections were placed on rhodium-plated Formvar-coated copper slot grids and mapped on the Phillips CM10 TEM at 80 kV, and then dual tilt series images were collected from +60° to –60° with 1° increments at 200 kV using a Tecnai 20 field emission gun (FEL; Beaverton, OR). Tomograms were imaged at 29,000× with a 0.77-nm pixel resolution (binning 2). Sections were coated on both sides with 15-nm fiducial gold for reconstruction of back projections using IMOD software (Kremer *et al.*, 1996). 3dmod software was used for mapping structure surface areas. Mean z-scale values for wild-type and *rsp5^{G555D}* sections were within 3%. Best-fit sphere models were used to measure vesicle diameters to the outer leaflet of membrane bilayers. IMOD calculated limiting membrane surface areas using three-dimensional (3D) mesh structures derived from closed contours drawn each 3.85 nm using imodmesh.

Affinity Isolation of Recombinant Proteins in Vitro

Liquid cultures (500 ml) of the *E. coli* strain BL21(DE3) transformed with the Codon Plus IL plasmid (Stratagene, La Jolla, CA) and transformed with pET-His PL or pGEX-4T1 expression vectors were grown to logarithmic phase in a shaking water bath at 37°C, and then incubated for 20 min in a shaking water bath at 20°C. On addition of 0.5 mM isopropyl- β -D-thiogalactopyranoside, the cultures were incubated an additional 16–20 h at 20°C and then harvested by centrifugation at 4500 × *g* for 5 min at 4°C. Pelleted cells that had been transformed with pET-HIS PL expression vectors were resuspended in ice-cold phosphate-buffered saline (PBS; 140 mM NaCl, 2.7 mM KCl, 10 mM Na₂HPO₄, 1.8 mM KH₂PO₄, pH 7.65) containing 1 mM phenylmethylsulfonyl fluoride (PMSF), 10 mM 2-mercaptoethanol, 20 mM imidazole, and 1 mg/ml lysozyme, and then incubated on ice for 30 min before being subjected to sonication. The lysates were clarified of cell debris by centrifugation at 15,000 × *g* for 5 min at 4°C, followed by centrifugation at 25,000 × *g* for 10 min at 4°C. Talon Cobalt affinity resin (Clontech, San Jose, CA) was added to the resulting supernatant, which was then rotated for 1 h at 4°C, and then washed three times with binding buffer (lysis buffer without lysozyme or PMSF). The His₆ fusion proteins were subsequently eluted from the resin with PBS, pH 8.0 containing 250 mM imidazole.

Pelleted cells that had been transformed with pGEX-4T1 expression vectors were resuspended in ice-cold Tris-buffered saline (TBS; 0.5 M NaCl, 20 mM Tris-HCl, pH 7.5), 1.0% Triton X-100, 1 mM PMSF, and 1 mg/ml lysozyme and then incubated on ice for 30 min before being subjected to sonication. The lysates were clarified of cell debris as described above, and the resulting supernatants were filtered through a 0.45- μ m pore size poly(vinylidene difluoride) membrane (Millipore, Bedford, MA) before passage through a GSTrap FF 5-ml column (GE Healthcare) equilibrated with TBS. After washing the column with 25 ml TBS, GST fusion proteins were eluted with 50 mM Tris-HCl, pH 8.0, containing 10 mM reduced glutathione.

Each isolated GST and His₆ fusion protein was assessed for its relative purity and concentration by SDS-PAGE and staining with Coomassie Brilliant Blue. Protein-binding assays were performed by adding pairwise combinations of the His₆ and GST fusion proteins (5 μ g of each) to binding buffer (390 mM NaCl, 2.7 mM KCl, 10 mM Na₂HPO₄, 1.8 mM KH₂PO₄, pH 7.4, 0.1% Triton X-100, 0.5% bovine serum albumin) to achieve a final volume of 500 μ l, which was rotated at 4°C for 1 h. Afterward, 25 μ l glutathione-Sepharose affinity resin (equilibrated in binding buffer) was added, and the mixture was rotated for 1 h at 4°C. The resin was then isolated by centrifugation at 10,000 \times g for 2 min at 4°C, washed three times with ice-cold binding buffer, washed twice with ice-cold PBS, and dried by centrifugation under vacuum. The sample was then resuspended in protein sample buffer, resolved by SDS-PAGE, and observed by staining with Coomassie Brilliant Blue.

RESULTS

Rsp5 Mediates Polyubiquitination of Sna3

Ub-independent sorting of Sna3 via the MVB pathway was originally demonstrated by fluorescence microscopic localization of GFP fused to a mutant form of Sna3 in which its only two cytosolic lysine residues (K₁₉ and K₁₂₅; Figure 1A) had been substituted with arginine (Reggiori and Pelham, 2001). However, Sna3 was recently identified in two independent yeast proteomic studies as a substrate for polyubiquitination (Hitchcock *et al.*, 2003; Peng *et al.*, 2003). Therefore, we investigated whether Sna3-GFP is modified by Ub attachment en route to the vacuole. Western blot analysis using anti-GFP antiserum detected both the full-length fusion protein (~48 kDa) and free GFP (~25 kDa) in extracts of wild-type cells expressing Sna3-GFP (Figure 1B). GFP cleavage from Sna3 was blocked when activation of vacuolar proteases was prevented by deletion of the *PEP4* gene (*pep4* Δ), indicating that cleavage of Sna3-GFP occurred upon its delivery into the vacuole lumen (Figure 1B). Higher molecular-weight forms of full-length Sna3-GFP were also detected in extracts of *pep4* Δ cells (Figure 1B, asterisks). Consistent with these forms being due to polyubiquitination, their abundance was significantly increased upon replacement of the wild-type *DOA4* gene with the catalytically inactive *doa4*^{C571S} allele (Figure 1B), indicating that the majority of Sna3-GFP is normally deubiquitinated by Doa4. Indeed, overexpression of wild-type *DOA4* eliminated the higher molecular-weight forms of Sna3-GFP observed in extracts of *pep4* Δ cells (Figure 1C). These forms corresponded to polyubiquitination of Sna3 rather than GFP because a similar pattern of modification was observed in extracts of *pep4* Δ *doa4*^{C571S} cells expressing Sna3 fused to HA, and overexpression of Myc-tagged Ub, which is slightly larger than wild-type Ub, caused each of the higher molecular-weight forms of Sna3-HA to appear as a doublet (Figure 1D).

Sna3-GFP localized to the vacuole lumen of both wild-type cells and *doa4*^{C571S} mutant cells (Figure 1E), consistent with previous work showing that Sna3 does not require Doa4 in order to be sorted via the MVB pathway (Reggiori and Pelham, 2001). In contrast, the *doa4*^{C571S} mutation caused CPS to accumulate in its ubiquitinated form (Figure 1B) and resulted in mislocalization of GFP-CPS to the vacuole membrane (Figure 1E). Thus, despite being polyubiquitinated, MVB sorting of Sna3 is not dependent on deubiquitination, unlike CPS and other Ub-dependent MVB

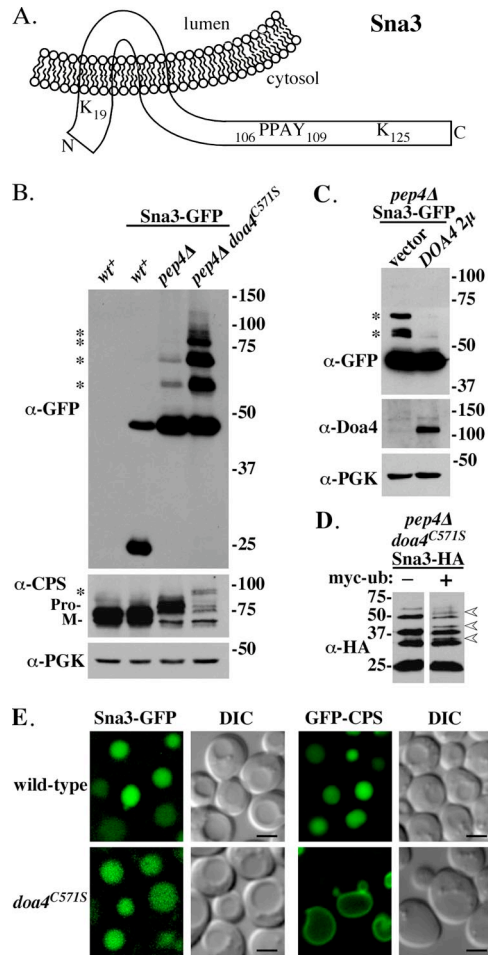


Figure 1. Sna3 is polyubiquitinated. (A) Schematic diagram of Sna3 indicating its orientation in the membrane and the locations of K₁₉, K₁₂₅, and the PPAY motif spanning amino acids 106-109. The N-terminal cytosolic domain of Sna3 consists of amino acids 1-21, and its C-terminal cytosolic domain consists of amino acids 64-133. (B) Western blot analysis of extracts prepared from wild-type cells (SEY6210), *pep4* Δ cells (TVY1), and *pep4* Δ *doa4*^{C571S} cells (MMY6) transformed with empty low-copy vector (pRS416) or with pRS416 encoding Sna3-GFP (*pSNA3-GFP*; Katzmam *et al.*, 2004). Asterisks indicate ubiquitinated forms of Sna3-GFP and CPS. PGK was examined as a control to indicate loading of equivalent lysate amounts. The reduced intensity of CPS in *pep4* Δ *doa4*^{C571S} extracts compared with wild-type and *pep4* Δ extracts might be due to the fact that, in *pep4* Δ *doa4*^{C571S} cells, some of the total pool of CPS is monoubiquitinated and some is not. (C) Western blot analysis of extracts prepared from *pep4* Δ *SNA3-GFP* cells (MMY161) transformed either with empty high-copy vector (pRS202) or pRS202 encoding wild-type *DOA4* (pGO289; Luhtala and Odorizzi, 2004). Asterisks indicate ubiquitinated forms of Sna3-GFP. Note that the low endogenous expression of Doa4 is difficult to detect. (D) Western blot analysis of extracts prepared from *pep4* Δ *doa4*^{C571S} *SNA3-HA* cells (MMY64) that had been transformed either with empty low-copy vector (pRS414) or pRS414 encoding Myc-Ub (pUB223; Berset *et al.*, 2002) and incubated with 250 μ M CuSO₄ to induce overexpression of Myc-Ub. Unmodified full-length Sna3-HA migrates at ~25 kDa. Equivalent loading of each extract was confirmed by blotting for PGK (data not shown). In B-D, antibodies used for Western blotting are indicated on the left, and the migration of molecular weight standards (kDa) are indicated on the right. Blotting of the samples shown in B with anti-Ub antibodies confirmed that Sna3-HA was polyubiquitinated. (E) Fluorescence and DIC microscopy of wild-type cells (SEY6210) and *doa4*^{C571S} cells (GOY100) transformed with *pSNA3-GFP* or a high-copy vector encoding GFP-CPS (pGO47; Odorizzi *et al.*, 1998). Bar, 2.5 μ m.

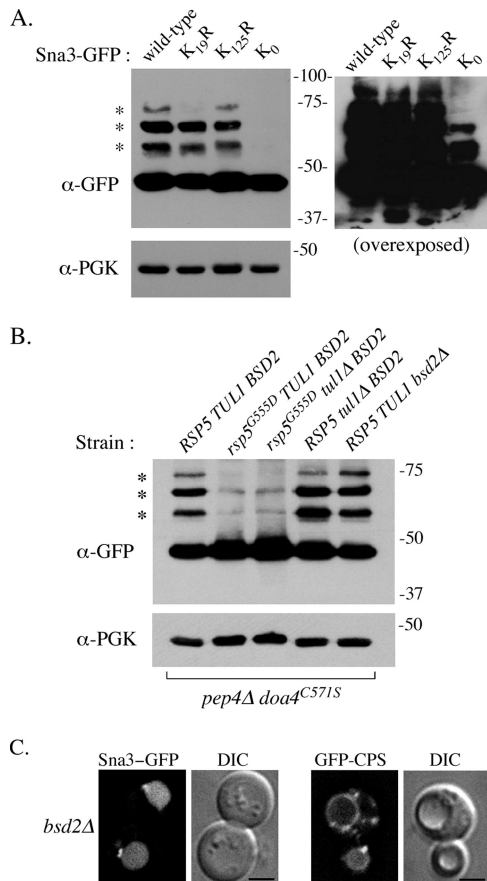


Figure 2. Rsp5 mediates polyubiquitination at either K₁₉ or K₁₂₅ of Sna3. (A) Western blot analysis of extracts prepared from *pep4Δ doa4^{C571S} sna3Δ* cells (MMY153) transformed with wild-type pSNA3-GFP or mutantized pSNA3-GFP in which arginine was substituted for K₁₉ (pMM158), K₁₂₅ (pMM152), or both K₁₉ and K₁₂₅ (K₀; pMM159). (B) Western blot analysis of extracts prepared from *pep4Δ doa4^{C571S} RSP5 TUL1 BSD2* cells (MMY64), *pep4Δ doa4^{C571S} rsp5^{G555D} TUL1 BSD2* cells (MMY127), *pep4Δ doa4^{C571S} rsp5^{G555D} tul1Δ BSD2* cells (MMY157), *pep4Δ doa4^{C571S} RSP5 tul1Δ BSD2* cells (GOY155), or *pep4Δ doa4^{C571S} RSP5 TUL1 bsd2Δ* (GOY157) cells transformed with pSNA3-GFP. In A and B, antibodies used for Western blotting are indicated on the left, and the migration of molecular weight standards (kDa) are indicated on the right. (C) Fluorescence and DIC microscopy of *bsd2Δ* cells (MMY56) transformed with pSNA3-GFP or pGO47. Bar, 2.5 μm.

cargoes (Dupre and Haguenaer-Tsapis, 2001; Katzmann *et al.*, 2001; Losko *et al.*, 2001).

Polyubiquitination of Sna3-GFP was not significantly affected by substitution of arginine in place of either K₁₉ or K₁₂₅ but was dramatically reduced upon simultaneous replacement of both K₁₉ and K₁₂₅ (K₀; Figure 2A). Higher molecular-weight forms of the K₀ mutant Sna3-GFP fusion protein could be faintly detected upon prolonged exposure (Figure 2A), raising the possibility that the N terminus of Sna3 can serve as an alternative site of ubiquitination (Ciechanover and Ben-Saadon, 2004). However, these data indicate that polyubiquitination of Sna3 predominantly occurs at either of its two cytosolic lysine residues.

Ubiquitination of most MVB cargo proteins in yeast requires Rsp5, a member of the HECT domain family of E3 Ub ligases (Blondel *et al.*, 2004; Dunn *et al.*, 2004; Hetteima *et al.*, 2004; Katzmann *et al.*, 2004; Morvan *et al.*, 2004). In addition, ubiquitination of at least some MVB cargoes involves Tul1,

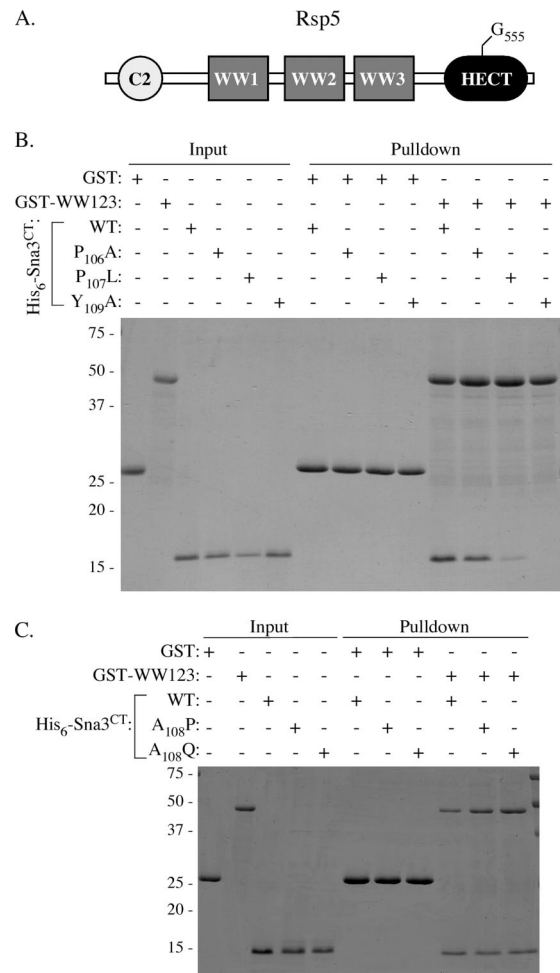


Figure 3. The PPAY motif of Sna3 mediates direct binding to Rsp5 WW domains. (A) Schematic diagram of Rsp5 indicating the positions of its C2 domain, three WW domains, and catalytic HECT domain, including amino acid G₅₅₅ important for ubiquitination of MVB cargoes (Katzmann *et al.*, 2004). (B and C) Coomassie-stained gels containing input amounts and glutathione-Sepharose pull-downs of the indicated recombinant fusion proteins expressed in bacteria and purified by affinity isolation. Inputs correspond to 50% of the amount of each recombinant protein used for pull-downs. GST was fused to the N terminus of a segment of Rsp5 containing all three of its WW domains (WW123; pIM2). His₆ was fused to a peptide corresponding to the wild-type C-terminal cytosolic domain of Sna3 (His₆-Sna3^{CT} WT; pMM143) or to the same peptide sequence containing the P₁₀₆A, P₁₀₇L, Y₁₀₉A, A₁₀₈P, or A₁₀₈Q substitutions (pMM168, pMM154, pMM169, pMM204, or pMM205, respectively). In B and C, the migration of molecular-weight standards (kDa) are indicated on the left.

a putative member of the RING domain family of E3 ligases (Reggiori and Pelham, 2002). Therefore, we examined how the loss of Rsp5 or Tul1 activity in *pep4Δ doa4^{C571S}* cells affects the polyubiquitination status of Sna3-GFP. As shown in Figure 2B, Ub modification of Sna3-GFP was severely impaired upon replacement of wild-type RSP5 with the *rsp5^{G555D}* mutant allele encoding a disabled Rsp5 enzyme that has reduced (but not eliminated) activity toward MVB cargo proteins (Katzmann *et al.*, 2004). The lower level of polyubiquitinated Sna3-GFP resulting from the *rsp5^{G555D}* mutation was not further decreased by simultaneous deletion of the TUL1 gene (*tul1Δ*), and the *tul1Δ* mutation alone had no effect (Figure 2B). Polyubiquitination of Sna3, there-

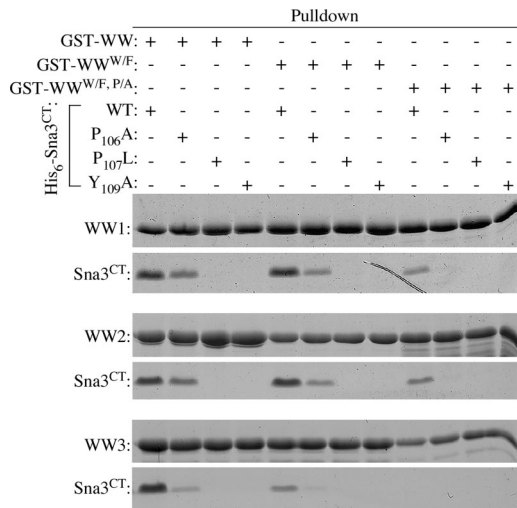


Figure 4. Binding of Sna3 to individual WW domains of Rsp5. Coomassie-stained gel containing glutathione-Sepharose pull-downs of the indicated recombinant fusion proteins expressed in bacteria and purified by affinity isolation. GST was fused to the N terminus of a segment of Rsp5 containing each individual wild-type WW domain (WW1, WW2, or WW3; pIM6, pIM10, or pIM8, respectively) or to each WW domain in which the WxxP motif was mutated by replacement of tryptophan with phenylalanine (W/F; pIM35, pIM36, or pIM37 for WW1, WW2, or WW3, respectively) or replacement of both tryptophan and proline with phenylalanine and alanine, respectively (W/F, P/A; pIM38, pIM39, or pIM40 for WW1, WW2, or WW3, respectively). The His₆-Sna3^{CT} are described in the legend to Figure 3. Migration of molecular weight standards (kDa) are indicated on the left.

fore, is mediated by Rsp5 and not Tul1. However, Rsp5 activity toward Sna3 does not require Bsd2, which serves as an adaptor protein that couples Rsp5 to certain types of MVB cargoes, including CPS (Hettema *et al.*, 2004; Stimpson *et al.*, 2006), because the level of polyubiquitinated Sna3-GFP is unaffected by deletion of the *BSD2* gene (*bsd2Δ*; Figure 2B). In addition, Sna3-GFP was correctly sorted via the MVB pathway in *bsd2Δ* mutant cells, unlike GFP-CPS, which was mislocalized in the absence of Bsd2 (Figure 2C).

The PPxY Motif of Sna3 Mediates Direct Binding to Rsp5 WW Domains

In addition to its catalytic HECT domain, Rsp5 contains a phospholipid-binding C2 domain and three WW domains (Figure 3A). The WW domains of Rsp5 bind directly to PPxY or PxY amino acid sequences located in a variety of proteins (Chang *et al.*, 2000). The presence of a PPxY motif in the C-terminal cytosolic domain of Sna3 (Figure 1A) raised the possibility that this sequence mediates direct association with Rsp5. Indeed, a hexahistidine (His₆)-tagged peptide corresponding to the C-terminal cytosolic domain of Sna3 (Sna3^{CT}) was isolated using glutathione-Sepharose affinity resin when mixed with glutathione S-transferase (GST) fused to a segment of Rsp5 that encompassed all three of its WW domains (WW123) but not when mixed with GST alone (Figure 3B). The binding between His₆-Sna3^{CT} and GST-WW123 was slightly decreased by mutation of P₁₀₆ in Sna3 but was more reduced by mutation of P₁₀₇ and completely eliminated by mutation of Y₁₀₉ (Figure 3B). In contrast, mutation of A₁₀₈ had no apparent effect on the binding of His₆-Sna3^{CT} to GST-WW123 (Figure 3C), consistent with the binding site for Rsp5 WW domains conforming to the PPxY consensus sequence.

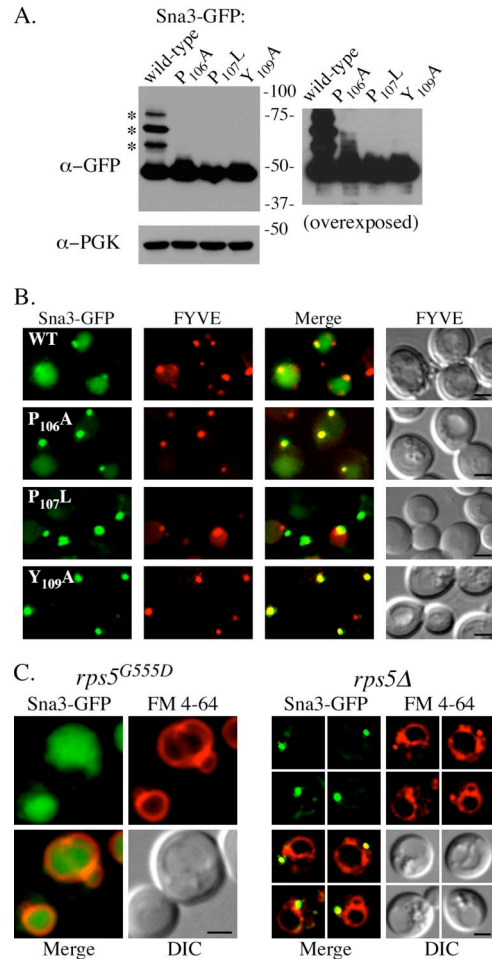


Figure 5. The PPAY motif is required for polyubiquitination and MVB sorting of Sna3-GFP. (A) Western blot analysis of extracts prepared from *pep4Δ doa4^{C571S} sna3Δ* cells (MMY153) transformed with wild-type pSNA3-GFP or mutagenized pSNA3-GFP containing the P₁₀₆A, P₁₀₇L, or Y₁₀₉A substitutions (pMM172, pMM99, or pMM171, respectively). Asterisks indicated ubiquitinated forms of Sna3-GFP. Antibodies used for blotting are indicated below each blot, and the migration of molecular weight standards (kDa) are indicated on the right. (B) Fluorescence and DIC microscopy of *sna3Δ* cells (MMY107) transformed with a high-copy vector encoding DsRed-FYVE (pRS425MET3-DsRed-FYVE; Katzmann *et al.*, 2003) and with wild-type pSNA3-GFP or mutagenized pSNA3-GFP containing the P₁₀₆A, P₁₀₇L, or Y₁₀₉A substitutions (pMM172, pMM99, or pMM171, respectively). Bar, 2.5 μm. (C) Fluorescence and DIC microscopy of FM 4-64-stained *rps5^{G555D}* cells (*mvb326*) or *rps5Δ* cells (GW003) transformed with pSNA3-GFP. Bar, 2.5 μm. Because Rsp5 is required for oleic acid synthesis, which is essential for viability in yeast (Hoppe *et al.*, 2000), *rps5Δ* cells were provided supplemental oleic acid in the growth medium.

Sna3 displayed no preference among the WW domains of Rsp5, because His₆-Sna3^{CT} bound with similar affinity to each individual WW domain fused to GST (Figure 4). However, the P₁₀₆ mutation in His₆-Sna3^{CT}, which had only a modest effect on binding to all three WW domains in tandem (Figure 3B), caused a strong reduction in binding to either WW1, WW2, or WW3 (Figure 4). Binding to each individual WW domain was completely eliminated by the P₁₀₇ mutation in His₆-Sna3^{CT}, and no interaction with individual WW domains occurred upon mutation of Y₁₀₉ (Figure 4), which was not surprising given that this mutation also completely disabled binding to GST-WW123 (Figure 3B).

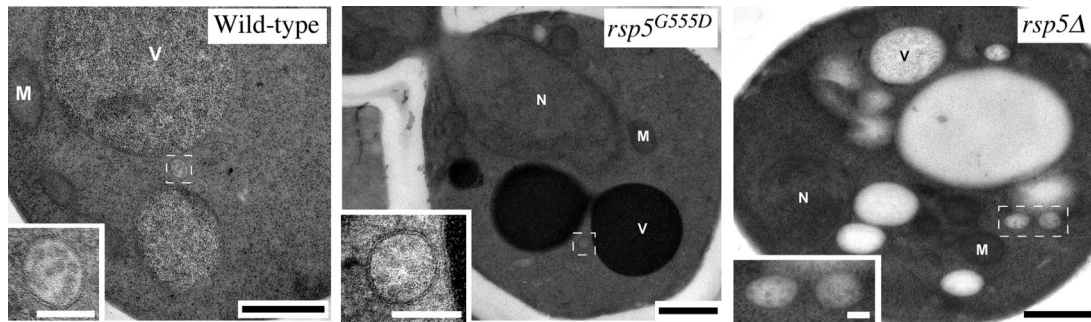


Figure 6. Rsp5 is not required for MVB biogenesis. Thin sections (~ 70 nm) of wild-type (SEY6210), *rsp5^{G555D}* (*mvb326*), and *rsp5 Δ* (GW003) cells were examined by EM at 80 kV. White scale bars, 100 nm; black scale bars, 500 nm.

Each WW domain in Rsp5 has a WxxP motif important for its interaction with PPxY sequences (Dunn and Hicke, 2001). Mutation of only the tryptophan residue in this motif had no effect on the ability of either WW1 or WW2 to bind His₆-Sna3^{CT}, whereas the interaction with WW3 was almost entirely lost (Figure 4). However, simultaneous mutation of both the tryptophan and proline residues of the WxxP motif significantly reduced the binding of WW1 and WW2 to His₆-Sna3^{CT} and eliminated binding of WW3 (Figure 4). The double mutation also disrupted the ability of WW1 and WW2 to interact with the P₁₀₆A mutant His₆-Sna3^{CT} (Figure 4). Together, the *in vitro* binding studies indicate that the PPxY sequence in the C-terminal cytosolic domain of Rsp5 interacts with each WW domain in Rsp5, although its interaction with WW1 and WW2 occurs with higher affinity than does its interaction with WW3.

The PPxY Motif Is Essential for Polyubiquitination and MVB Sorting of Sna3

Binding of Rsp5 to the PPxY motif *in vivo* is required for polyubiquitination of Sna3, as mutation of either P₁₀₇ or Y₁₀₉ eliminated Ub modification of Sna3-GFP (Figure 5A). Ubiquitination of Sna3-GFP was also greatly decreased by mutation of P₁₀₆ but could be faintly detected in longer exposures (Figure 5A), consistent with the *in vitro* binding studies indicating that the interaction between Rsp5 and Sna3 was reduced but not eliminated upon mutation of P₁₀₆ (Figure 3B). Notably, the PPxY motif was also required for sorting of Sna3 via the MVB pathway. As shown in Figure 5B, Sna3-GFP was not delivered into the vacuole lumen upon mutation of Y₁₀₉ and, instead, localized exclusively to punctate structures that were also labeled by DsRed fused to the FYVE domain, which binds to phosphatidylinositol 3-phosphate enriched in endosomal membranes (Burd and Emr, 1998; Gaullier *et al.*, 1998). Previous studies showed that wild-type Sna3-GFP was similarly excluded from vacuoles and accumulated at endosomal compartments upon disruption of class E Vps protein functions (Reggiori and Pelham, 2001; Yeo *et al.*, 2003; Katzmann *et al.*, 2004), a condition in which sorting of all MVB cargoes is blocked (Odorizzi *et al.*, 1998). However, mutation of P₁₀₆ in Sna3-GFP resulted in an intermediate phenotype in which a portion of the fusion protein was located in the vacuole lumen in addition to being localized to endosomes (Figure 5B), again consistent with P₁₀₆ having a less important role in MVB sorting. In fact, wild-type Sna3-GFP occasionally also colocalized with DsRed-FYVE at punctate structures in addition to being localized within the vacuole lumen (Figure 5B). Mutation of P₁₀₇ in contrast, resulted in a stronger mutant phenotype than that caused by the P₁₀₆ mutation in that Sna3-GFP was

excluded from the vacuole lumen in the majority of cells (Figure 5B).

Previous work showed that sorting of Sna3 via the MVB pathway was not affected by mutations that disable Rsp5 catalytic activity (Katzmann *et al.*, 2004). Accordingly, Sna3-GFP was correctly localized within the vacuole lumen in *rsp5^{G555D}* cells (Figure 5C), and electron microscopy (EM) analysis of thin cell sections confirmed that the *rsp5^{G555D}* mutation does not block MVB vesicle formation (Figure 6). In contrast, Sna3-GFP was excluded from the vacuole of *rsp5 Δ* cells (Figure 5C), consistent with MVB sorting of Sna3 being dependent on its direct association with Rsp5. The punctate structures in *rsp5 Δ* cells at which Sna3-GFP was localized were also stained by FM 4-64 (Figure 5C), a fluorescent lipophilic dye that intercalates into the plasma membrane and is transported via the endocytic pathway to the vacuole (Vida and Emr, 1995). Labeling of the vacuole membrane in *rsp5 Δ* cells by FM 4-64 ruled out the possibility that transport to the vacuole is generally blocked in cells lacking Rsp5 expression. Moreover, EM analysis of *rsp5 Δ* cells indicated that Rsp5 is not essential for MVB vesicle formation (Figure 6), although the vacuoles of *rsp5 Δ* lacked electron density, suggesting that the absence of Rsp5 expression impacts vacuolar function.

Loss of Rsp5 Catalytic Activity Affects MVB Vesicle Size

For a closer study of MVB morphology, we examined thick sections of cells by dual-axis tomography, which provides structural information in three dimensions and at a higher resolution than can be achieved from thin sections (McIntosh *et al.*, 2005). A 5-nm section derived from tomographic reconstruction of an MVB representative of >60 examined by tomography in wild-type cells is shown in Figure 7A, and the 3D tomogram of this MVB is available as Supplementary Video 1. As inferred from EM analysis of thin sections (Figure 6), tomography showed that the limiting MVB membrane is approximately spherical and surrounds numerous luminal vesicles. Modeling of the MVB shown in Figure 7A revealed that the diameters of the MVB vesicles were not uniform but, instead, ranged between 22 and 35 nm (Figure 7C; also available as Supplementary Video 2). This relatively broad distribution of MVB vesicle sizes was evident when we plotted the diameters of 330 vesicles derived from tomographic reconstructions of 13 MVBs in wild-type cells (Figure 7E).

An MVB representative of >20 examined by tomography in *rsp5^{G555D}* cells is shown in Figure 7B and modeled in Figure 7D (also available as Supplementary Videos 3 and Video 4, respectively). However, a comparable tomographic analysis of MVB morphology in *rsp5 Δ* cells was not possible

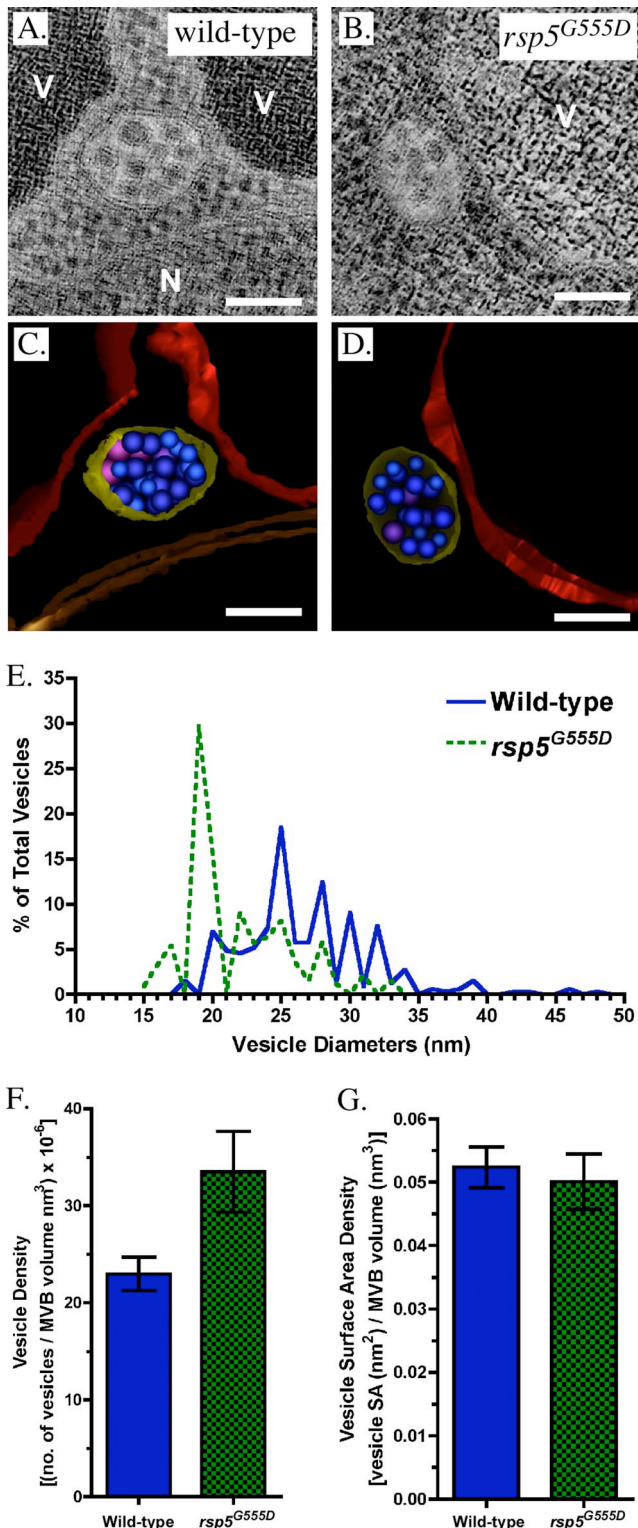


Figure 7. Tomographic analysis of MVB morphology. Two-dimensional cross sections and 3D models derived from 200-nm-thick section tomograms of wild-type (SEY6210; A and B) and *rsp5^{G555D}* cells (*mbv326*; C and D). See corresponding Supplementary Videos. V, vacuole; N, nucleus. Scale bars, 100 nm. The luminal vesicles in modeled MVBs are color-coded based on diameter (aqua, 18–23 nm; blue, 24–29 nm; bluish purple, 30–35 nm; purple, 36–41). (E) Distribution of vesicle diameters in wild-type and *rsp5^{G555D}* cells ($n = 330$ and 333, respectively) normalized as percent of total. (F) Density of vesicles per unit luminal MVB volume (nm³) in wild-type and

because the lack of electron density in the vacuoles of this strain caused distortions of the electron beam transmission. The most striking feature of the MVB in Figure 7, B and D (and others observed in *rsp5^{G555D}* cells) was that it contained more small vesicles and fewer large vesicles. The shift toward smaller vesicles in *rsp5^{G555D}* cells was indicated when we plotted the diameters of 333 vesicles derived from tomographic reconstruction of 17 MVBs in this strain (Figure 7E). This change in the distribution of differently sized vesicles in *rsp5^{G555D}* cells versus wild-type cells suggests that Rsp5 activity influences the formation of MVB vesicles even though analysis of *rsp5 Δ* cells showed that Rsp5, per se, is not required for this process to occur (Figure 6). However, the shift in the vesicle size distribution in *rsp5^{G555D}* cells was not due to elimination of larger vesicles from the total pool of luminal MVB vesicles. On the contrary, the total number of vesicles per MVB actually increased in *rsp5^{G555D}* cells (Figure 7F). Overall, the surface area represented by luminal vesicles in wild-type and *rsp5^{G555D}* cells was approximately equal (Figure 7G). The increased number of small MVB vesicles in *rsp5^{G555D}* cells, therefore, presumably has the same total carrying capacity as MVB vesicles in wild-type cells.

DISCUSSION

Most integral membrane proteins in yeast require monoubiquitination of their cytosolic domains in order to be sorted into the MVB pathway. Monoubiquitin is recognized as an MVB sorting signal by Ub-binding subunits of the class E Vps/ESCRT machinery (reviewed in Hicke and Dunn, 2003; Hurley and Emr, 2006). Sorting of Snz3, however, is Ub-independent because its delivery into the vacuole lumen is not impaired by substituting both of its cytosolic lysine residues with arginine (Reggiori and Pelham, 2001) or by mutations that either disable the cycle of MVB cargo ubiquitination and deubiquitination (Reggiori and Pelham, 2001; Katzmann *et al.*, 2004) or prevent Ub binding by class E Vps proteins (Bilodeau *et al.*, 2002). Here, we show that Snz3 circumvents the need for Ub by interacting directly with Rsp5, the E3 Ub ligase primarily responsible for monoubiquitination of yeast MVB cargoes (Blondel *et al.*, 2004; Dunn *et al.*, 2004; Hettema *et al.*, 2004; Katzmann *et al.*, 2004; Morvan *et al.*, 2004).

Rsp5 functions in multiple Ub-dependent protein trafficking steps, including endocytosis, Golgi-to-endosome transport, and MVB cargo sorting (reviewed in Dupre *et al.*, 2004). Recruitment of Rsp5 to endosomes is mediated in part by its C2 domain, which binds to phosphoinositides, including phosphatidylinositol 3-phosphate enriched in endosomal membranes (Dunn *et al.*, 2004). Like Snz3, Rsp5 colocalizes with DsRed-FYVE at endosomes (Katzmann *et al.*, 2004) and is trapped at late endosomal membranes in cells lacking functional Vps4 (Dunn *et al.*, 2004), the ATPase that catalyzes dissociation of class E Vps proteins from endosomes (Hurley and Emr, 2006). Although the precise spatial relationship between Rsp5 and the class E Vps machinery is unknown, our observation that direct association with Rsp5 is required for sorting Snz3 into the MVB pathway suggests that Rsp5 is

rsp5^{G555D} cells ($p < 0.05$, unpaired t test). (G) Vesicle surface area density (nm²) per unit luminal MVB volume (nm³) in wild-type and *rsp5^{G555D}* cells ($p = 0.69$, unpaired t test). The same data sets for wild-type and *rsp5^{G555D}* cells were used to generate the graphs in E–G.

located in the vicinity of endosomal membrane microdomains where class E Vps proteins function in the sequestration and packaging of MVB cargoes into lumenal vesicles. The coordination of Rsp5 with class E Vps proteins is also consistent with previous work showing that sorting of Sna3 into the MVB pathway requires the class E Vps machinery (Reggiori and Pelham, 2001), indicating that Sna3 is transported via the same route used by Ub-dependent cargoes.

Other examples of Ub-independent MVB cargo sorting have been described, including the Cvt17 protein in yeast and the δ -opioid receptor in humans. As in the case of Sna3, class E Vps proteins are required for sorting Cvt17 and δ -opioid receptor via the MVB pathway (Epple *et al.*, 2001; Tanowitz and Von Zastrow, 2002; Hislop *et al.*, 2004), but how these cargoes gain access to the sorting machinery is unknown. Surprisingly, class E Vps proteins are not essential for sorting the human Pmel17 melanosomal protein into lumenal vesicles. Moreover, sorting of Pmel17 relies on sequences in its lumenal domain rather than its cytosolic domain (Theos *et al.*, 2006), although the molecular basis for its recognition as an MVB cargo is unclear.

We have shown that recognition of Sna3 as an MVB cargo requires the PPAY sequence located in its C-terminal cytosolic domain, which mediates direct binding to the WW domains of Rsp5. In a parallel study (Oestreich *et al.*, 2007), the PPAY of Sna3 was shown to be both necessary and sufficient for mediating MVB sorting when transplanted onto the cytosolic domain of a membrane protein not normally transported via the MVB pathway. PPxY or PxY motifs are common binding sites for WW domains in Rsp5 (Chang *et al.*, 2000) and in the Nedd4 family of HECT domain E3 Ub ligases in mammalian cells, which are homologues of Rsp5 (Ingham *et al.*, 2004). Notably, several types of enveloped viruses encode structural proteins containing PPxY motifs that bind Nedd4 and bud from infected cells by a process that is both topologically equivalent to MVB vesicle budding and is dependent on the functions of class E Vps proteins (Harty *et al.*, 2000; Bouamr *et al.*, 2003; Gottwein *et al.*, 2003; Martin-Serrano *et al.*, 2004; Vana *et al.*, 2004; Segura-Morales *et al.*, 2005; reviewed in Morita and Sundquist, 2004). Like Rsp5, Nedd4 proteins function in ubiquitination of cargoes sorted into the MVB pathway (Staub *et al.*, 1997; Marchese *et al.*, 2003), but whether ubiquitination of viral proteins by Nedd4 is directly required for packaging of viral particles is unclear (Morita and Sundquist, 2004). PPxY-containing viral proteins might be concentrated at sites of viral assembly through their direct interaction with Nedd4 proteins. Indeed, one member of the Nedd4 family stably associates with Tsg101, a subunit of ESCRT-I (Medina *et al.*, 2005), indicating a physical link exists between the E3 Ub ligase and core MVB sorting components. Recently, Rsp5 was found to bind directly to Hse1, a subunit of the ESCRT-0 complex (Ren *et al.*, 2006), which might explain how Sna3 bound to Rsp5 gains access to the class E Vps/ESCRT MVB sorting machinery.

The residual polyubiquitination of Sna3-GFP detected upon mutation of both of its cytosolic lysines or upon its expression in *rsp5^{G555D}* cells leaves open the possibility that low level ubiquitination of Sna3 is sufficient for mediating MVB sorting. Oestreich *et al.* (2007) found that polyubiquitination of Sna3 occurred at its N terminus if both cytosolic lysines were mutated, but blocking N-terminal ubiquitination did not prevent the lysine-deficient mutant Sna3 from being sorted via the MVB pathway. Combined with our study, this result strongly suggests that polyubiquitination of Sna3 has no role in its MVB sorting but is most likely the result of its direct association with Rsp5. Indeed, most

models regarding the mechanism of polyubiquitin chain assembly assume continuous association of an E3 ligase with the substrate during multiple rounds of Ub addition (Hochstrasser, 2006). In contrast, monoubiquitination can occur through transient or indirect E3-substrate interactions, as exemplified by Nedd4 in mammalian cells, which can monoubiquitinate substrates in the absence of any detectable physical interaction (Polo *et al.*, 2002). Unlike Sna3, monoubiquitinated cargoes in yeast may encounter Rsp5 stochastically because of their colocalization at endosomal microdomains rather than rely on sequence-specific motifs that mediate direct association with Rsp5 (Dunn *et al.*, 2004).

Recruitment of Rsp5 to sites where certain types of cargoes concentrate is mediated by Bsd2, a transmembrane protein containing a PPxY motif that binds directly to Rsp5 WW domains (Hettema *et al.*, 2004). Bsd2 functions as an adaptor that directs Rsp5 activity toward proteins (such as CPS) that contain polar amino acids in their transmembrane domains (Hettema *et al.*, 2004; Stimpson *et al.*, 2006). Sna3 does not contain polar residues in either of its two transmembrane domains, consistent with our results indicating that neither its polyubiquitination nor its MVB sorting require Bsd2. Like Sna3, the PPxY motif in Bsd2 mediates its association with Rsp5 WW domains and its sorting via the MVB pathway (Hettema *et al.*, 2004). Although the function of Sna3 is unknown, its similarity to Bsd2 suggests it could mediate recruitment of Rsp5 to sites where certain types of MVB cargoes are concentrated.

Previous observations of the Ub-independent sorting of Sna3 into the MVB pathway implied that the role of Ub is restricted to ESCRT-mediated recognition of cargoes such as CPS (Reggiori and Pelham, 2001; Bilodeau *et al.*, 2002; Katzmann *et al.*, 2004). 3D electron tomography, however, suggests that the Ub ligase activity of Rsp5 influences MVB vesicle formation because there was a higher frequency of smaller vesicles in *rsp5^{G555D}* cells compared with the broader distribution MVB vesicle sizes seen in wild-type cells. Although the size of an MVB vesicle might be related to the amount of cargoes it transports, the total surface area represented by lumenal vesicles was equivalent in wild-type and *rsp5^{G555D}* cells. Nevertheless, most yeast proteins require ubiquitination to be recognized as MVB cargoes (Hicke and Dunn, 2003). Future work might reveal why an equal capacity for MVB transport is maintained in *rsp5^{G555D}* cells and might also provide insight into how Ub influences the size of MVB vesicles.

ACKNOWLEDGMENTS

We thank Megan Wemmer (University of Colorado, Boulder) for strain construction, Stefan Lanker (Oregon Health Sciences University) for providing pUB223, Scott Emr (University of California, San Diego) for providing pSNA3-GFP and yeast strain *mb326*, and David Katzmann (Mayo Foundation, Rochester, MN) for communication of unpublished results. This work was supported by a grant to G.O. from the American Cancer Society (RSG-02-147-01-CSM). M.W.M. is supported by a training grant from the National Institutes of Health (5 T32 GM-07135). G.O. is an Arnold and Mabel Beckman Foundation Young Investigator.

REFERENCES

- Berset, C., Griac, P., Tempel, R., La Rue, J., Wittenberg, C., and Lanker, S. (2002). Transferable domain in the G(1) cyclin Cln2 sufficient to switch degradation of Sic1 from the E3 ubiquitin ligase SCF(Cdc4) to SCF(Grr1). *Mol. Cell. Biol.* 22, 4463–4476.
- Bilodeau, P. S., Urbanowski, J. L., Winistorfer, S. C., and Piper, R. C. (2002). The Vps27p Hse1p complex binds ubiquitin and mediates endosomal protein sorting. *Nat. Cell Biol.* 4, 534–539.

- Blondel, M. O., Morvan, J., Dupre, S., Urban-Grimal, D., Haguenaer-Tsapis, R., and Volland, C. (2004). Direct sorting of the yeast uracil permease to the endosomal system is controlled by uracil binding and Rsp5p-dependent ubiquitylation. *Mol. Biol. Cell* 15, 883–895.
- Bouamr, F., Melillo, J. A., Wang, M. Q., Nagashima, K., de Los Santos, M., Rein, A., and Goff, S. P. (2003). PPPYVEPTAP motif is the late domain of human T-cell leukemia virus type 1 Gag and mediates its functional interaction with cellular proteins Nedd4 and Tsg101 [corrected]. *J. Virol.* 77, 11882–11895.
- Burd, C. G., and Emr, S. D. (1998). Phosphatidylinositol(3)-phosphate signaling mediated by specific binding to RING FYVE domains. *Mol. Cell* 2, 157–162.
- Chang, A., Cheang, S., Espanel, X., and Sudol, M. (2000). Rsp5 WW domains interact directly with the carboxyl-terminal domain of RNA polymerase II. *J. Biol. Chem.* 275, 20562–20571.
- Ciechanover, A., and Ben-Saadon, R. (2004). N-terminal ubiquitination: more protein substrates join in. *Trends Cell Biol.* 14, 103–106.
- Cowles, C. R., Snyder, W. B., Burd, C. G., and Emr, S. D. (1997). Novel Golgi to vacuole delivery pathway in yeast: identification of a sorting determinant and required transport component. *EMBO J.* 16, 2769–2782.
- Doyotte, A., Russell, M. R., Hopkins, C. R., and Woodman, P. G. (2005). Depletion of TSG101 forms a mammalian “Class E” compartment: a multicisternal early endosome with multiple sorting defects. *J. Cell Sci.* 118, 3003–3017.
- Dunn, R., and Hicke, L. (2001). Domains of the Rsp5 ubiquitin-protein ligase required for receptor-mediated and fluid-phase endocytosis. *Mol. Biol. Cell* 12, 421–435.
- Dunn, R., Klos, D. A., Adler, A. S., and Hicke, L. (2004). The C2 domain of the Rsp5 ubiquitin ligase binds membrane phosphoinositides and directs ubiquitination of endosomal cargo. *J. Cell Biol.* 165, 135–144.
- Dupre, S., and Haguenaer-Tsapis, R. (2001). Deubiquitination step in the endocytic pathway of yeast plasma membrane proteins: crucial role of Doa4p ubiquitin isopeptidase. *Mol. Cell Biol.* 21, 4482–4494.
- Dupre, S., Urban-Grimal, D., and Haguenaer-Tsapis, R. (2004). Ubiquitin and endocytic internalization in yeast and animal cells. *Biochim. Biophys. Acta* 1695, 89–111.
- Epple, U. D., Suriapranata, I., Eskelinen, E. L., and Thumm, M. (2001). Aut5/Cvt17p, a putative lipase essential for disintegration of autophagic bodies inside the vacuole. *J. Bacteriol.* 183, 5942–5955.
- Futter, C. E., Pearce, A., Hewlett, L. J., and Hopkins, C. R. (1996). Multivesicular endosomes containing internalized EGF-EGF receptor complexes mature and then fuse directly with lysosomes. *J. Cell Biol.* 132, 1011–1023.
- Gaullier, J. M., Simonsen, A., D’Arrigo, A., Bremnes, B., Stenmark, H., and Aasland, R. (1998). FYVE fingers bind PtdIns(3)P. *Nature* 394, 432–433.
- Gottwein, E., Bodem, J., Muller, B., Schmechel, A., Zentgraf, H., and Krausslich, H. G. (2003). The Mason-Pfizer monkey virus PPPY and PSAP motifs both contribute to virus release. *J. Virol.* 77, 9474–9485.
- Guthrie, C., and Fink, G. R. (eds.) (2002). *Guide to yeast genetics and molecular biology*. San Diego: Academic Press.
- Harty, R. N., Brown, M. E., Wang, G., Huibregtse, J., and Hayes, F. P. (2000). A PPxY motif within the VP40 protein of Ebola virus interacts physically and functionally with a ubiquitin ligase: implications for filovirus budding. *Proc. Natl. Acad. Sci. USA* 97, 13871–13876.
- Hettema, E. H., Valdez-Taubas, J., and Pelham, H. R. (2004). Bsd2 binds the ubiquitin ligase Rsp5 and mediates the ubiquitination of transmembrane proteins. *EMBO J.* 23, 1279–1288.
- Hicke, L., and Dunn, R. (2003). Regulation of membrane protein transport by ubiquitin and ubiquitin-binding proteins. *Annu. Rev. Cell Dev. Biol.* 19, 141–172.
- Hislop, J. N., Marley, A., and Von Zastrow, M. (2004). Role of mammalian vacuolar protein-sorting proteins in endocytic trafficking of a non-ubiquitinated G protein-coupled receptor to lysosomes. *J. Biol. Chem.* 279, 22522–22531.
- Hitchcock, A. L., Auld, K., Gygi, S. P., and Silver, P. A. (2003). A subset of membrane-associated proteins is ubiquitinated in response to mutations in the endoplasmic reticulum degradation machinery. *Proc. Natl. Acad. Sci. USA* 100, 12735–12740.
- Hochstrasser, M. (2006). Lingering mysteries of ubiquitin-chain assembly. *Cell* 124, 27–34.
- Hoppe, T., Matuschewski, K., Rape, M., Schlenker, S., Ulrich, H. D., and Jentsch, S. (2000). Activation of a membrane-bound transcription factor by regulated ubiquitin/proteasome-dependent processing. *Cell* 102, 577–586.
- Horadzovsky, B. F., Busch, G. R., and Emr, S. D. (1994). VPS21 encodes a rab5-like GTP binding protein that is required for the sorting of yeast vacuolar proteins. *EMBO J.* 13, 1297–1309.
- Hurley, J. H., and Emr, S. D. (2006). The ESCRT complexes: structure and mechanism of a membrane-trafficking network. *Annu. Rev. Biophys. Biomol. Struct.* 35, 277–298.
- Ingham, R. J., Gish, G., and Pawson, T. (2004). The Nedd4 family of E3 ubiquitin ligases: functional diversity within a common modular architecture. *Oncogene* 23, 1972–1984.
- Katzmann, D. J., Babst, M., and Emr, S. D. (2001). Ubiquitin-dependent sorting into the multivesicular body pathway requires the function of a conserved endosomal protein sorting complex, ESCRT-I. *Cell* 106, 145–155.
- Katzmann, D. J., Sarkar, S., Chu, T., Audhya, A., and Emr, S. D. (2004). Multivesicular body sorting: ubiquitin ligase Rsp5 is required for the modification and sorting of carboxypeptidase S. *Mol. Biol. Cell* 15, 468–480.
- Katzmann, D. J., Stefan, C. J., Babst, M., and Emr, S. D. (2003). Vps27 recruits ESCRT machinery to endosomes during MVB sorting. *J. Cell Biol.* 162, 413–423.
- Kremer, J. R., Mastronarde, D. N., and McIntosh, J. R. (1996). Computer visualization of three-dimensional image data using IMOD. *J. Struct. Biol.* 116, 71–76.
- Longtine, M. S., McKenzie, A., 3rd, Demarini, D. J., Shah, N. G., Wach, A., Brachat, A., Philippsen, P., and Pringle, J. R. (1998). Additional modules for versatile and economical PCR-based gene deletion and modification in *Saccharomyces cerevisiae*. *Yeast* 14, 953–961.
- Losko, S., Kopp, F., Kranz, A., and Kolling, R. (2001). Uptake of the ATP-binding cassette (ABC) transporter Ste6 into the yeast vacuole is blocked in the doa4 mutant. *Mol. Biol. Cell* 12, 1047–1059.
- Luhtala, N., and Odorizzi, G. (2004). Bro1 coordinates deubiquitination in the multivesicular body pathway by recruiting Doa4 to endosomes. *J. Cell Biol.* 166, 717–729.
- Lykke-Andersen, J., Shu, M. D., and Steitz, J. A. (2000). Human Upf proteins target an mRNA for nonsense-mediated decay when bound downstream of a termination codon. *Cell* 103, 1121–1131.
- Macias, M. J., Wiesner, S., and Sudol, M. (2002). WW and SH3 domains, two different scaffolds to recognize proline-rich ligands. *FEBS Lett.* 513, 30–37.
- Marchese, A., Raiborg, C., Santini, F., Keen, J. H., Stenmark, H., and Benovic, J. L. (2003). The E3 ubiquitin ligase AIP4 mediates ubiquitination and sorting of the G protein-coupled receptor CXCR4. *Dev. Cell* 5, 709–722.
- Martin-Serrano, J., Perez-Caballero, D., and Bieniasz, P. D. (2004). Context-dependent effects of L domains and ubiquitination on viral budding. *J. Virol.* 78, 5554–5563.
- McIntosh, R., Nicastro, D., and Mastronarde, D. (2005). New views of cells in 3D: an introduction to electron tomography. *Trends Cell Biol.* 15, 43–51.
- Medina, G., Zhang, Y., Tang, Y., Gottwein, E., Vana, M. L., Bouamr, F., Leis, J., and Carter, C. A. (2005). The functionally exchangeable L domains in RSV and HIV-1 Gag direct particle release through pathways linked by Tsg101. *Traffic* 6, 880–894.
- Morita, E., and Sundquist, W. I. (2004). Retrovirus budding. *Annu. Rev. Cell Dev. Biol.* 20, 395–425.
- Morvan, J., Froissard, M., Haguenaer-Tsapis, R., and Urban-Grimal, D. (2004). The ubiquitin ligase Rsp5p is required for modification and sorting of membrane proteins into multivesicular bodies. *Traffic* 5, 383–392.
- Mullock, B. M., Bright, N. A., Fearon, C. W., Gray, S. R., and Luzio, J. P. (1998). Fusion of lysosomes with late endosomes produces a hybrid organelle of intermediate density and is NSF dependent. *J. Cell Biol.* 140, 591–601.
- Odorizzi, G., Babst, M., and Emr, S. D. (1998). Fab1p PtdIns(3)P 5-kinase function essential for protein sorting in the multivesicular body. *Cell* 95, 847–858.
- Odorizzi, G., Katzmann, D. J., Babst, M., Audhya, A., and Emr, S. D. (2003). Bro1 is an endosome-associated protein that functions in the MVB pathway in *Saccharomyces cerevisiae*. *J. Cell Sci.* 116, 1893–1903.
- Oestreich, A. J., Aboian, M., Lee, J., Azmi, I., Payne, J., Issaka, R., Davies, B. A., and Katzmann, D. J. (2007). Characterization of multiple multivesicular body sorting determinants within Sna3: a role for the ubiquitin ligase Rsp5. *Mol. Biol. Cell* 18, 707–720.
- Peng, J., Schwartz, D., Elias, J. E., Thoreen, C. C., Cheng, D., Marsischky, G., Roelofs, J., Finley, D., and Gygi, S. P. (2003). A proteomics approach to understanding protein ubiquitination. *Nat. Biotechnol.* 21, 921–926.
- Polo, S., Sigismund, S., Faretta, M., Guidi, M., Capua, M. R., Bossi, G., Chen, H., De Camilli, P., and Di Fiore, P. P. (2002). A single motif responsible for

- ubiquitin recognition and monoubiquitination in endocytic proteins. *Nature* 416, 451–455.
- Reggiori, F., and Pelham, H. R. (2001). Sorting of proteins into multivesicular bodies: ubiquitin-dependent and -independent targeting. *EMBO J.* 20, 5176–5186.
- Reggiori, F., and Pelham, H. R. (2002). A transmembrane ubiquitin ligase required to sort membrane proteins into multivesicular bodies. *Nat. Cell Biol.* 4, 117–123.
- Ren, J., Kee, Y., Huibregtse, J. M., and Piper, R. C. (2006). Hse1, a component of the yeast Hrs-STAM ubiquitin sorting complex, associates with ubiquitin peptidases and a ligase to control sorting efficiency into multivesicular bodies. *Mol. Biol. Cell* 18, 324–335.
- Rieder, S. E., Banta, L. M., Kohrer, K., McCaffery, J. M., and Emr, S. D. (1996). Multilamellar endosome-like compartment accumulates in the yeast vps28 vacuolar protein sorting mutant. *Mol. Biol. Cell* 7, 985–999.
- Robinson, J. S., Kliensky, D. J., Banta, L. M., and Emr, S. D. (1988). Protein sorting in *Saccharomyces cerevisiae*: isolation of mutants defective in the delivery and processing of multiple vacuolar hydrolases. *Mol. Cell. Biol.* 8, 4936–4948.
- Sambrook, J., and Russell, D. (2001). *Molecular cloning: a laboratory manual*. Woodbury, NY: Cold Spring Harbor Laboratory Press.
- Segura-Morales, C., Pescia, C., Chatellard-Causse, C., Sadoul, R., Bertrand, E., and Basyuk, E. (2005). Tsg101 and Alix interact with murine leukemia virus Gag and cooperate with Nedd4 ubiquitin ligases during budding. *J. Biol. Chem.* 280, 27004–27012.
- Sikorski, R. S., and Hieter, P. (1989). A system of shuttle vectors and yeast host strains designed for efficient manipulation of DNA in *Saccharomyces cerevisiae*. *Genetics* 122, 19–27.
- Staub, O., Gautschi, I., Ishikawa, T., Breitschopf, K., Ciechanover, A., Schild, L., and Rotin, D. (1997). Regulation of stability and function of the epithelial Na⁺ channel (ENaC) by ubiquitination. *EMBO J.* 16, 6325–6336.
- Stimpson, H. E., Lewis, M. J., and Pelham, H. R. (2006). Transferrin receptor-like proteins control the degradation of a yeast metal transporter. *EMBO J.* 25, 662–672.
- Tanowitz, M., and Von Zastrow, M. (2002). Ubiquitination-independent trafficking of G protein-coupled receptors to lysosomes. *J. Biol. Chem.* 277, 50219–50222.
- Theos, A. C., Truschel, S. T., Tenza, D., Hurbain, I., Harper, D. C., Berson, J. F., Thomas, P. C., Raposo, G., and Marks, M. S. (2006). A luminal domain-dependent pathway for sorting to intraluminal vesicles of multivesicular endosomes involved in organelle morphogenesis. *Dev. Cell* 10, 343–354.
- Urbanowski, J. L., and Piper, R. C. (2001). Ubiquitin sorts proteins into the intraluminal degradative compartment of the late-endosome/vacuole. *Traffic* 2, 622–630.
- van Deurs, B., Holm, P. K., Kayser, L., and Sandvig, K. (1995). Delivery to lysosomes in the human carcinoma cell line HEP-2 involves an actin filament-facilitated fusion between mature endosomes and preexisting lysosomes. *Eur. J. Cell Biol.* 66, 309–323.
- Vana, M. L., Tang, Y., Chen, A., Medina, G., Carter, C., and Leis, J. (2004). Role of Nedd4 and ubiquitination of Rous sarcoma virus Gag in budding of virus-like particles from cells. *J. Virol.* 78, 13943–13953.
- Vida, T. A., and Emr, S. D. (1995). A new vital stain for visualizing vacuolar membrane dynamics and endocytosis in yeast. *J. Cell Biol.* 128, 779–792.
- Wang, G., McCaffery, J. M., Wendland, B., Dupre, S., Haguenaer-Tsapis, R., and Huibregtse, J. M. (2001). Localization of the Rsp5p ubiquitin-protein ligase at multiple sites within the endocytic pathway. *Mol. Cell Biol.* 21, 3564–3575.
- Winey, M., Mamay, C. L., O'Toole, E. T., Mastronarde, D. N., Giddings, T. H., Jr., McDonald, K. L., and McIntosh, J. R. (1995). Three-dimensional ultrastructural analysis of the *Saccharomyces cerevisiae* mitotic spindle. *J. Cell Biol.* 129, 1601–1615.
- Wurmser, A. E., and Emr, S. D. (1998). Phosphoinositide signaling and turnover: PtdIns(3)P, a regulator of membrane traffic, is transported to the vacuole and degraded by a process that requires luminal vacuolar hydrolase activities. *EMBO J.* 17, 4930–4942.
- Yeo, S. C. *et al.* (2003). Vps20p and Vta1p interact with Vps4p and function in multivesicular body sorting and endosomal transport in *Saccharomyces cerevisiae*. *J. Cell Sci.* 116, 3957–3970.